JOURNAL OF APPLIED ELECTROCHEMISTRY 21 (1991) 64–72

The effect of Co^{2+}, Cu^{2+}, Fe^{2+} and Fe^{3+} during electrowinning of nickel

S. K. GOGIA, S. C. DAS

Regional Research Laboratory, Bhubaneswar 751013, India

Received 12 October 1989; revised 15 March 1990

The effects of the impurities Co^{2+}, Cu^{2+}, Fe^{2+}, Fe^{3+} on the current efficiency, physical appearance, purity, crystallographic orientation and surface morphology of the deposit and on nickel deposition polarization behaviour during nickel electrowinning were determined. The current efficiency did not change significantly in the presence of these impurities over the concentration range studied, but certain changes in the purity and physical appearance of the deposit were observed. Based on the physical appearance of the electrodeposited nickel, the tolerance limits of the impurities in the electrolyte are reported. The tolerance limit of Co^{2+} was a maximum at 500 p.p.m. and a minimum at 5 p.p.m. in the case of Fe^{2+}. No deviation of nickel structure from fcc was observed in the presence of any of these impurities but the peak height values for different orientations showed variations with all the impurities and the values also changed with increase in the impurity concentrations. The surface morphology of electrodeposited nickel also changed in the presence of the impurities. The potentiodynamic scan curves for electrodeposition of nickel showed deviations in the presence of all the impurities except Cu^{2+}. Based on the results, an attempt is made to correlate the effects of the various factors investigated.

1. Introduction

The electrodeposition of nickel has been studied by several investigators with respect to current efficiency, polarization behaviour and deposit structural characteristics [1–17]. Some attempts have been made to correlate the brightness of the nickel deposit with structural variations [18–23]. In all these studies, a sulphate-chloride or sulphamate bath as such or with additives was used. A literature survey indicates that little information [24–36] is available on the effect of several common impurities (both cations and anions) during electrodeposition of nickel. Nickel baths, including the bright plating baths, are very sensitive to impurities such as Mg, Cu, Zn, Cr, etc. and sulphur-containing organic compounds [33]. These impurities, besides increasing the tendency of pitting, may change the characteristics of the deposit. Recently Das and Gogia [37] studied the effect of Mg, Mn, Al and Zn during electrodeposition of nickel. They observed that although these impurities did not affect current efficiency significantly, they had an appreciable effect on the purity, physical appearance and structural characteristics of the deposits as well as on the polarization.

In the present paper, the results of a systematic study on the effect of Co^{2+}, Cu^{2+}, Fe^{2+} and Fe^{3+} during nickel electrowinning are reported. During the study, the effects of these impurities on the physical appearance, purity, crystalographic orientation and surface morphology of the deposit and on the polarization behaviour and current efficiency of nickel deposition were determined. An attempt was also made to correlate the effects of the various factors investigated.

2. Experimental details

2.1. *Apparatus and material*

A 500 ml beaker fitted with a porous refractory diaphragm was used as the electrowinning cell. Stainless steel and Pb–Sb (Sb 7%) sheets were used as cathodes and anodes, respectively. The cathode area was 100 mm^2.

The electrolytic solution was prepared from nickel sulphate, boric acid and sodium sulphate. Its pH was adjusted by adding sulphuric acid. In order to study the effects of impurities, the respective sulphates were used. All the chemicals were of AnalaR grade and the solutions were prepared from distilled water.

2.2. *Electrolysis*

All the electrowinning experiments were carried out for 2 h at a current density of 400 A m^{-2} and at room temperature (30 ± 1° C). The electrolyte solution contained mainly 60 g dm^{-3} nickel and 12 g dm^{-3} each of boric acid and sodium sulphate. Impurity additions were made as aliquots from their respective stock solutions. After electrolysis the cathode was removed and thoroughly washed with water and acetone followed by drying. The cathodic current efficiency was calculated from the increased weight of the cathode.

0021-891X/90 $03.00 + .12

2.3. *Deposit analysis*

Photomacrographs were taken to examine the physical appearance of the deposit. For examining the contamination of the nickel deposits by impurities, the deposits were first analysed by optical emission spectrograph and EDAX and then quantitatively by atomic absorption spectroscopy (AAS). For these analyses, samples were collected randomly from different parts of the deposits (apart from the edges) and all the analyses were carried out in duplicate. The average value of the analyses are reported.

The surface morphology of the deposits was examined by SEM and to determine the preferred orientation relative to the ASTM standard for nickel powder, sections of the deposits were examined by X-ray diffraction (XRD).

2.4. *Polarization measurements*

Current-potential curves for nickel deposition were measured with a Wenking potentiostat (model ST 72) operated in the potentiostatic mode. The scan rate was maintained at $1\,mV\,s^{-1}$ controlled by a Wenking voltage scan generator (VSG 72). The cathode was a platinum sheet with a cross section of $1\,cm^2$ and freshly coated with a nickel layer deposited from a pure nickel bath. Each experiment was carried out with a freshly prepared cathode. The anode was also a platinum sheet having the same area as the cathode. The reference electrode was a saturated calomel electrode (SCE), separated from the test cell with a salt bridge containing the same electrolyte. The later terminated in a luggin probe, positioned very close to the cathode to minimize the *IR* drop. The effects of various impurities at different concentrations on the *i–V* curves were measured from -300 to $-900\,mV$ with respect to SCE.

3. Results and discussion

3.1. *Current efficiency*

At optimum conditions (Table 1) it was possible to achieve bright and smooth nickel deposit with close to 100% current efficiency. Under these conditions the individual effects of the impurities were studied and the results are reported in Table 2. It was observed that the current efficiency decreased in the presence of any of the impurities studied and that the effect was intensified at higher concentrations of the impurities.

Table 1. Optimum conditions for nickel electrowinning

Electrolyte	$60\,g\,dm^{-3}$ Ni $12\,g\,dm^{-3}$ H_3BO_3 $12\,g\,dm^{-3}$ Na_2SO_4
Bath pH	2.5
Temperature	$30 \pm 1°C$ (Room temperature)
Current density	$400\,A\,m^{-2}$
Diaphragm	Porous refractory
Duration	2 h
Current efficiency	> 99%

Table 2. Effect of impurities on current efficiency, contamination and physical appearance of the deposit during electrowinning of nickel

Electrolyte content (p.p.m.)		*Current efficiency (%)*	*Contamination (%)*	*Physical appearance*
Co^{2+}	100	99.54	0.38	Perfect sheet
	250	98.54	0.85	Perfect sheet
	500	97.94	1.72	Perfect sheet
	1000	96.50	3.15	Cracking, peeling
	2000	93.30	5.60	Cracking, peeling and granular deposition
Cu^{2+}	100	97.89	0.048	Perfect sheet
	250	97.36	0.85	Black spongy deposits on the bottom portion
	500	96.97	1.65	Increase of black spongy deposition
	1000	96.84	2.36	Dense black spongy deposition throughout the surface
Fe^{2+}	5	99.68	0.02	Perfect sheet
	10	99.56	0.03	Cracking and granular deposition
	20	99.44	0.11	do
	100	99.30	0.21	do
	250	98.30	0.39	More cracking and granular deposition
	1000	97.55	0.66	Granular deposition and cracking into pieces
Fe^{3+}	100	98.13	0.17	Perfect sheet
	250	98.74	0.28	Cracking and peeling
	500	98.69	1.00	More cracking and peeling

3.2. *Deposit quality*

Observations on the deposit quality, on addition of the impurities to the nickel electrolyte at different concentrations, are reported in Table 2 and Fig. 1. In general, cracking and peeling of the deposits and spongy or granular formation on the surface were observed. These effects were intensified at high impurity concentrations. The deposit quality of nickel did not change even up to 500 p.p.m. of Co^{2+}. But when the Co^{2+} concentration was increased to 1000 p.p.m. this caused the nickel sheet to crack and peel away. See Fig. 1b. Similar observations [32, 33] were also made during electrodeposition of Co–Ni alloy. The deterioration of the deposit was attributed to the greater internal stress developed during electrodeposition of the alloy. In the case of Cu^{2+}, even 250 p.p.m. caused formation of black nodular growth. On increase of Cu^{2+} concentration, the effect was intensified (Fig. 1c) and the nodular growth almost covered the entire surface when the concentration was increased to 1000 p.p.m. (Fig. 1d). As observed from the results, Fe^{2+} had the most deleterious effect on the nickel deposit with respect to its tolerance limit in the bath. Even low Fe^{2+} concentrations caused cracking of the

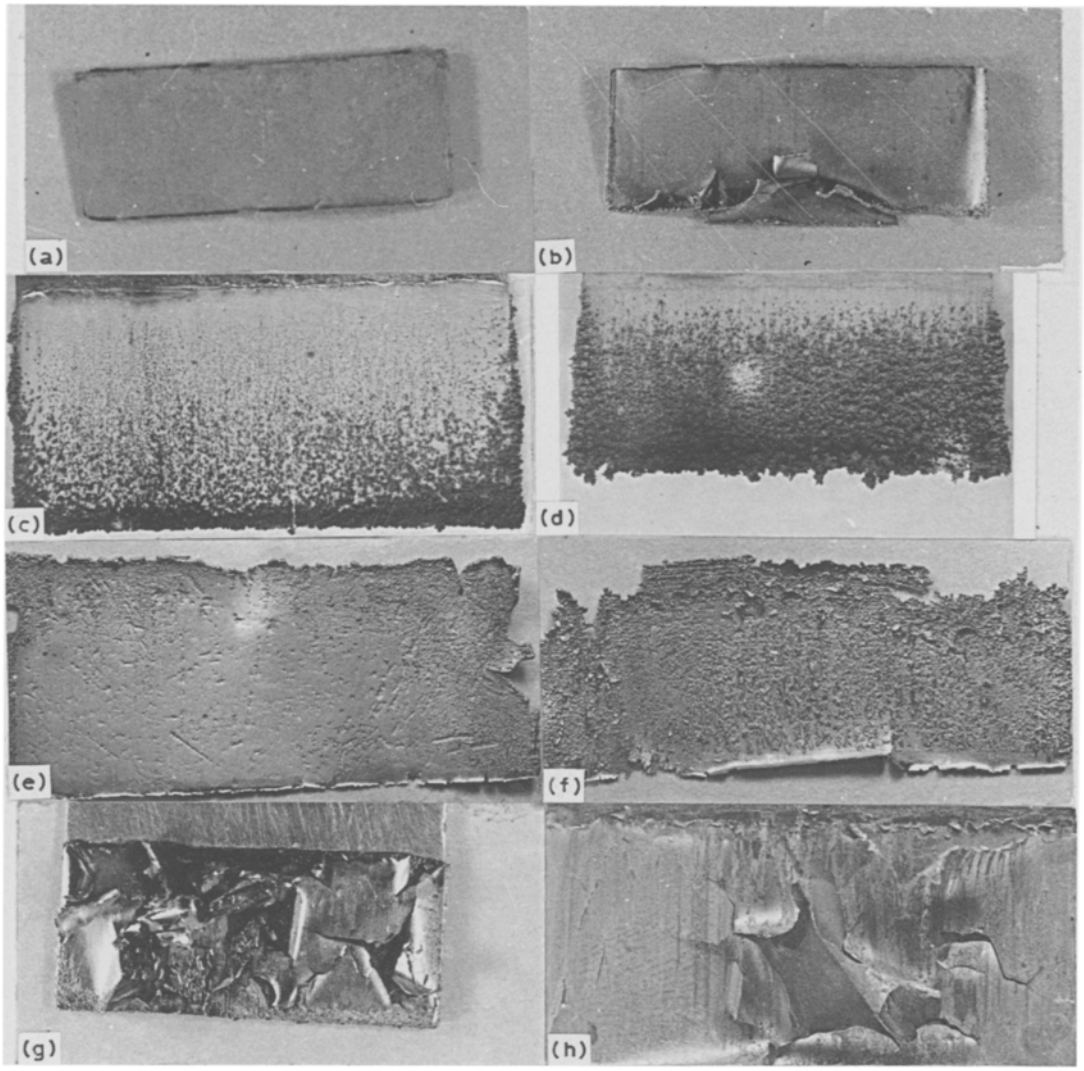

Fig. 1. Photographs showing the effect of impurities on the physical appearance of electrodeposited nickel: (a) without impurity; (b) 1000.p.p.m. Co; (c) 500 p.p.m. Cu; (d) 1000 p.p.m. Cu; (e) 20 p.p.m. Fe^{2+}; (f) 250 p.p.m. Fe^{2+}; (g) 250 p.p.m. Fe^{3+}; and (h) 500 p.p.m. Fe^{3+}

deposit and formation of granular deposition (Fig. 1e). Increase of Fe^{2+} concentration caused further deterioration of the physical appearance of the deposit. The presence of Fe^{3+} at low concentration was found to be comparatively less harmful than Fe^{2+}. The deposit quality was not affected until 100 p.p.m. of Fe^{3+}, but beyond this concentration, the deposit started cracking and peeling (Figs 1g and h). The formation of yellowish nickel deposits was observed when the concentrations of both Fe^{2+} and Fe^{3+} exceeded 100 p.p.m. This is probably due to the precipitation of $Fe(OH)_3$ or a basic salt at the surface [33, 36]. As observed from the present data, the nickel deposit started cracking and peeling when the concentrations of Fe^{2+} and Fe^{3+} exceeded 5 and 100 p.p.m., respectively. Similar observations were also reported in the literature [38]. The cracking and peeling of the nickel deposit due to the presence of iron were explained by Mellor [38] in the following manner. When a trace of iron is present it tends to deposit more readily on the cathode than nickel, so that the first layer contains a higher proportion of iron than subsequent layers. As a result, strain is set up and flaking occurs. Based on the deposit quality obtained in the presence of various impurities in the concentration range studied, their tolerance limits were reported in Table 3 along with the standard electrode potentials. It is found that the tolerance limits did not follow any sequence with standard electrode potentials as reported earlier [37].

3.3. *Deposit contamination*

Nickel deposits obtained in the presence of various impurities at different concentrations were analysed and the results are reported in Table 2. As observed, the deposits were contaminated with all the impurities studied. In general, the impurity concentration in the deposit increased with increase of bath concentration. The contamination was least in the case of Fe^{2+} and maximum in the case of Co^{2+}. Cobalt codeposits (as alloy) along with nickel, since its reduction potential is very close to that of nickel [32]. Further, Co^{2+} reduces to the metallic state in simple and acid solution at a lower deposition potential than nickel [33]. This explains the reason for more contamination of the nickel deposit with cobalt. The extent of contamination due to the presence of Cu^{2+} followed that of Co^{2+}. Being more noble, copper may deposit in preference to

Table 3. Tolerance limits of various impurities in the nickel bath

Impurities	*Tolerance limits (p.p.m.)*	*Contamination (%)*	*Standard electrode potential*	*Electrode reaction*
Ni^{2+}	–	–	−0.250	$Ni^{2+} + 2e \longrightarrow Ni$
Co^{2+}	500	1.72	−0.277	$Co^{2+} + 2e \longrightarrow Co$
Cu^{2+}	100	0.048	+0.33	$Cu^{2+} + 2e \longrightarrow Cu$
Fe^{2+}	5	0.02	−0.44	$Fe^{2+} + 2e \longrightarrow Fe$
Fe^{3+}	500	0.17	+0.771	$Fe^{3+} + e \longrightarrow Fe^{2+}$

nickel. The nickel deposit was also contaminated when Fe^{2+} was present in the bath. Further, the contamination increased with increase of Fe^{2+} bath concentration (i.e. 0.03% at 10 p.p.m. of Fe^{2+} and 0.66% at 1000 p.p.m. of Fe^{2+}). This may be due to anomalous codeposition of iron with nickel [33, 40]. Anomalous codeposition appears to be closely related to the local pH rise at the surface. Dahm [41, 42] hypothesized that this surface pH increase causes the formation of a ferrous hydroxide which suppresses the discharge of nickel. As observed from the data, this does not happen in the present case, because the current efficiency did not change significantly although iron concentration, both in the bath as well as in the deposit, increased (Table 2). An alternative mechanism for this anomalous codeposition was suggested by Nicol and Philip [43] who explained the codeposition of iron as being due to underpotential deposition. The present observation seems to support the mechanism proposed by Nicol and Philip [43]. The nickel deposit was found to be more contaminated in the presence of Fe^{3+} than Fe^{2+} at higher concentrations (> 250 p.p.m.) (Table 2). The contamination due to Fe^{3+} may take place through reduction of Fe^{3+} to Fe^{2+} followed by Fe^{2+} to Fe under the experimental conditions, or due to precipitation of $Fe(OH)_3$/basic salt and subsequent inclusion in the deposit or combination of both reduction of Fe^{3+} to Fe and precipitation reactions.

Table 4. Crystallographic orientations of nickel deposits as a function of impurities at different concentrations

Impurities	*Impurities concentration (p.p.m.)*	*Peak height (cm) orientation* (1 1 1)	(2 0 0)	(2 2 0)
	0	0.5	0.75	6.15
Co^{2+}	100	0.5	1.1	7.3
	500	0.3	0.7	4.5
	1000	0.4	0.75	6.6
Cu^{2+}	100	0.5	0.90	5.7
	250	0.3	0.65	6.9
	500	1.1	0.95	4.6
Fe^{2+}	10	0.6	1.0	4.7
	100	2.2	3.0	2.3
	250	2.1	0.9	5.6
Fe^{3+}	100	0.3	0.6	4.4
	500	0.6	0.6	2.8

3.4. *Crystallographic orientations*

The effects of impurities on the crystallographic orientations of electrodeposited nickel were determined by X-ray diffraction and the results are summarized in Table 4. The crystallographic orientations of the electrodeposited nickel obtained from the pure bath (Table 1) were found to be (1 1 1), (2 0 0) and (2 2 0). This indicated the nickel deposit to be a face centered cubic structure as reported by Yang [6] and Machu *et al.* [31]. No change in the structure of electrodeposited nickel was noted when any of these impurities were added to the bath. Similar observations were also reported by Machu *et al.* [31] and Das and Gogia [37] while electrodepositing nickel in the presence of some impurities. However, significant change in the peak height values for the different orientations (Table 4) were observed.

From the peak height values it is observed that lower Co^{2+} concentration in the bath favoured crystal growth in the direction of the (2 2 0) and (2 0 0) planes whereas higher concentrations favoured the growth of the (2 2 0) plane only; a decrease in all the peak height values was observed at intermediate Co^{2+} concentration. However, throughout the concentration range studied, the (2 2 0) orientation remained preferred. In the case of Cu^{2+}, although lower concentrations favoured the growth of the (2 0 0) orientation, higher concentrations favoured both (2 0 0) and (1 1 1) orientations, whereas promotion of crystal growth in the direction of the (2 2 0) plane was observed at intermediate Cu^{2+} concentration. As in the case of Co^{2+}, the (2 2 0) orientation remained preferred throughout. When Fe^{2+} was added to the nickel electrolyte, the peak height values for nickel deposits showed a different behaviour. The peak height values for the (1 1 1) and (2 0 0) orientations showed an abrupt increase at 100 p.p.m. of Fe^{2+} in the bath, whereas at 250 p.p.m. of Fe^{2+} similar behaviour was observed for the (2 2 0) orientation. Up to 100 p.p.m. Fe^{2+} the crystal growth was favoured in the directions of the (1 1 1) and (2 0 0) planes, whereas promotion of the (2 2 0) orientation was observed at 250 p.p.m. of Fe^{2+}. Although the (2 2 0) orientation remained preferred at both lower and higher Fe^{2+} concentrations, the preferred orientation for intermediate concentration (i.e. 100 p.p.m.) was observed to be the (2 0 0) plane. The crystallographic orientations of the deposit due to addition of Fe^{3+} to the bath were quite different from those obtained in

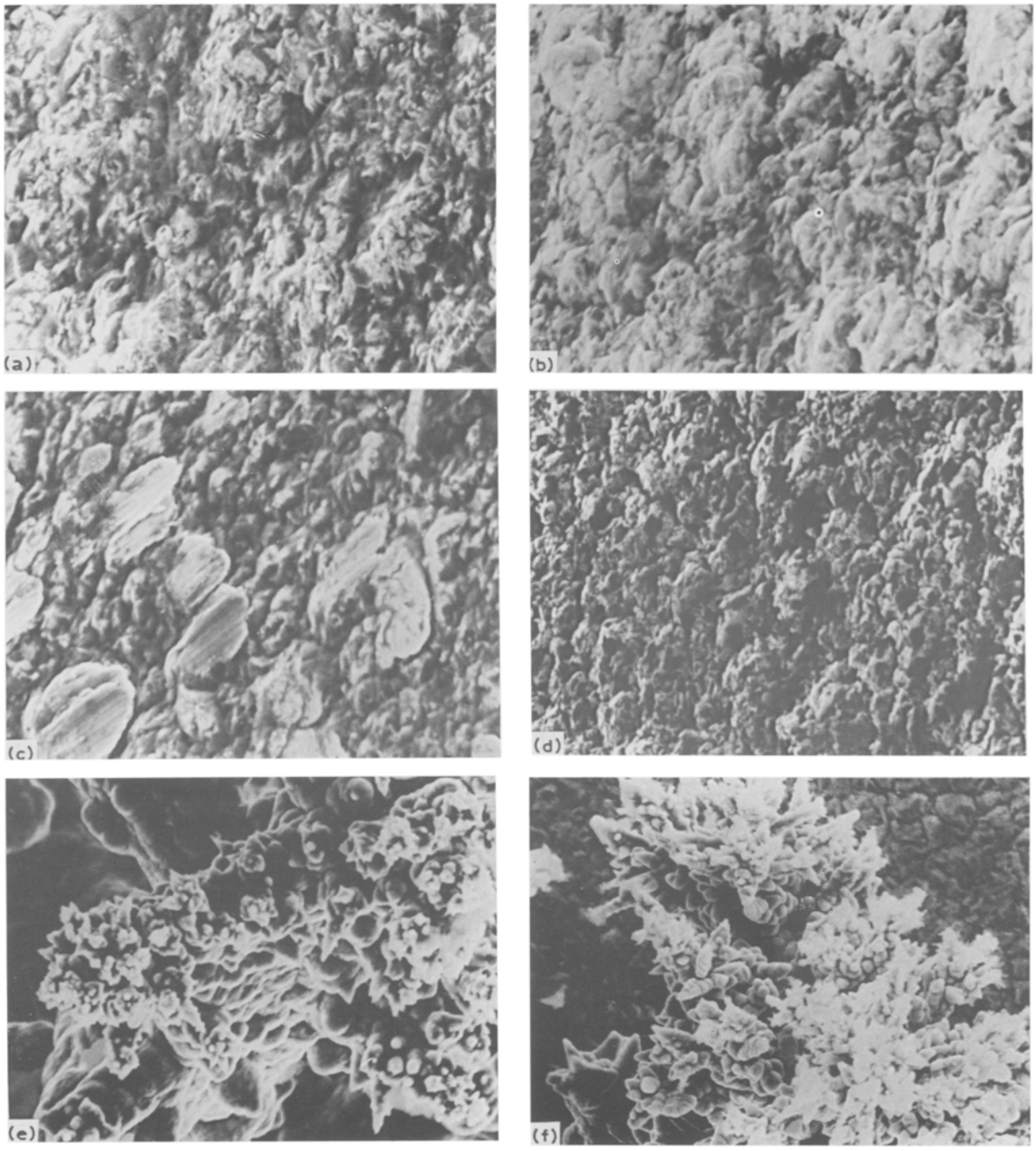

Fig. 2. SEM photomicrographs (× 1200) of nickel electrodeposits in the absence and presence of impurities: (a) without impurity; (b) 100 p.p.m. Co (c) 1000 p.p.m. Co; (d) 100 p.p.m. Cu (× 640); (e) 100 p.p.m. Cu; (f) 500 p.p.m. Cu.

the case of Fe^{2+}. In this case the peak height values for all the planes i.e. (1 1 1), (2 0 0) and (2 2 0) decreased at lower Fe^{3+} concentration. But when the concentration was increased by five times, the promotion of crystal growth in the (1 1 1) direction was observed. However, as in the cases of Co^{2+} and Cu^{2+}, the (2 2 0) orientation remained preferred throughout in the presence of Fe^{3+}.

3.5. *Surface morphology*

The surface morphology of the electrodeposited nickel from both pure and impurity-containing electrolytes were determined by SEM. Some typical photomicrographs are shown in Figs 2 and 3.

Fig. 2a shows the morphology of the nickel deposit obtained from the pure bath where randomly oriented fine shaped crystallites are located in the form of colonies. The morphological changes due to the presence of Co^{2+} in the bath are shown in Figs 2b and c. Addition of 100 p.p.m. of Co^{2+} to the bath not only increased the crystallite size but also increased the colony size, Fig. 2b. Moreover, the deposit seems to be more compact. Nodular block growth of different sizes, oriented at an angle $\sim 45°$ was observed when the Co^{2+} concentration was increased to 1000 p.p.m. Fig. 2c. Similar changes were also observed in crystal orientations. Addition of 100 p.p.m. Co^{2+} promoted the crystal growth in the direction of the (1 1 1) and (2 2 0) planes, whereas the

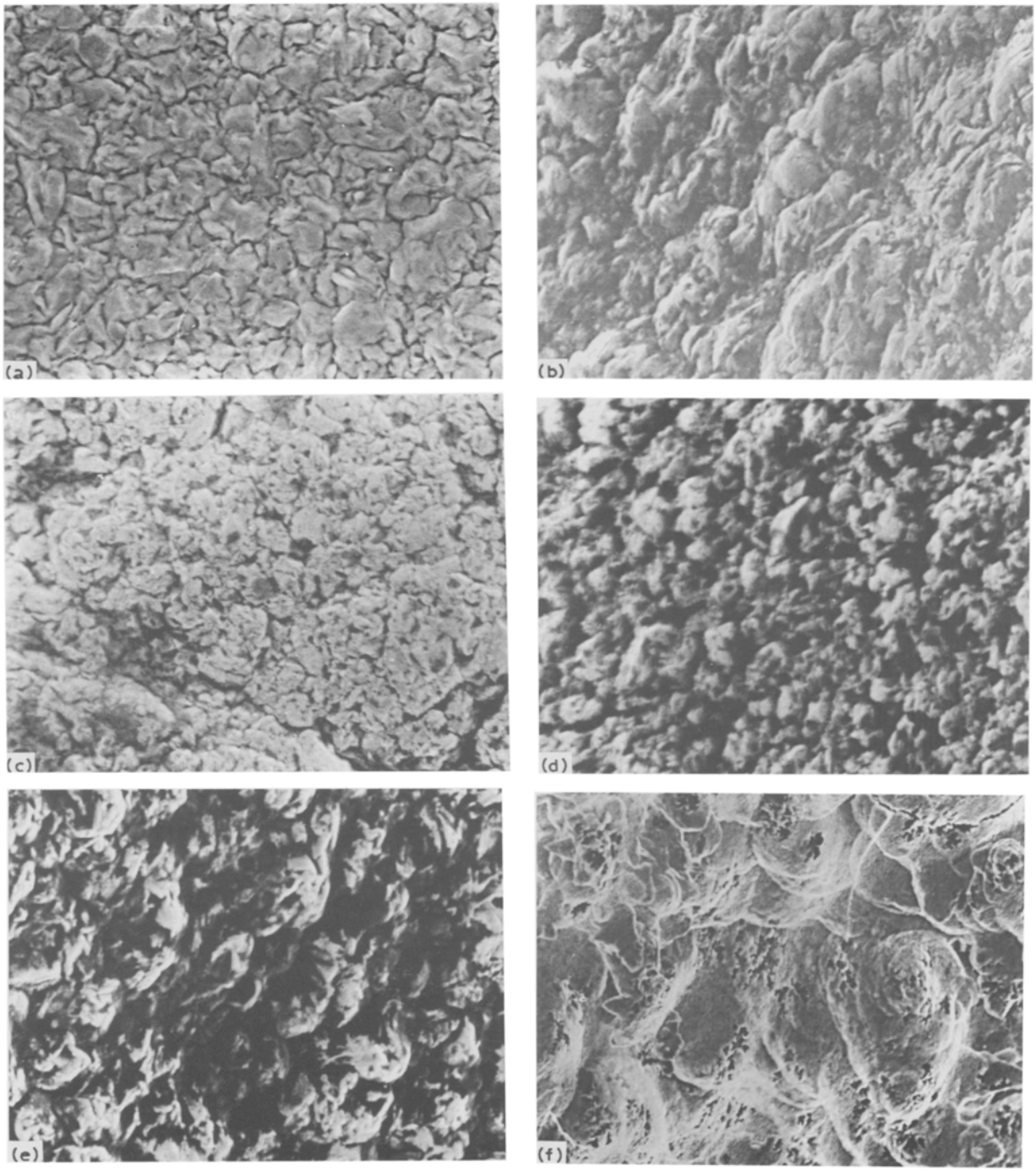

Fig. 3. SEM photomicrographs (× 1200) of nickel electrodeposits in the presence of impurities: (a) 500 p.p.m. Cu (× 1600); (b) 20 p.p.m. Fe^{2+}; (c) 100 p.p.m. Fe^{2+}; (d) 1000 p.p.m. Fe^{2+} (× 2000); (e) 100 p.p.m. Fe^{3+}; and (f) 500 p.p.m. Fe^{3+} (× 600).

growth was favoured only in the direction of the (2 2 0) orientation when the Co^{2+} concentration was increased to 1000 p.p.m..

Figs 2 and 3 show the deposit morphology in the presence of Cu^{2+} at two different concentrations. At both the concentrations the nodular portions of the deposits showed very poor morphology, Figs 2e and f. The morphology of the smoother portions of the deposits are shown in Figs 2d and 3a. At lower concentration the crystallite size increased and the crystallites were located in the form of colonies. At higher Cu^{2+} concentration the deposit had a completely different morphology. Such morphological changes were also reflected in the crystal orientations. At lower concentration the crystal growth was promoted in the direction of the (2 0 0) plane, whereas at the higher concentration the growth was favoured in the direction of the (1 1 1) and (2 0 0) planes. The nickel deposit morphology in the presence of Fe^{2+} are shown in Fig. 3.

The presence of Fe^{2+} in the electrolyte resulted in a totally different morphology. At low Fe concentration the crystallites were located in the form of colonies, Fig. 3b, and the deposit was relatively compact. But as the concentration approached 100 p.p.m. or above the morphology of the nickel deposits changed and the crystallites were located in the form of clusters. As the Fe^{2+} in the electrolyte increased a decrease in the

cluster size was also observed. The observed morphological changes were accompanied by changes in crystal orientation and the physical appearance of the deposit, as reported in earlier sections. Marked changes in the crystallite size and shape were also observed for deposits obtained from Fe^{3+} containing electrolyte. An almost similar morphology was obtained at both lower and higher Fe^{3+} concentrations, Figs 3e and f.

3.6. *Polarization behaviour*

Potentiodynamic scan curves for electrodeposition of nickel in the presence of impurities such as Co^{2+}, Cu^{2+}, Fe^{2+} and Fe^{3+} at different concentrations were recorded. The results are reported in Figs 4 and 5.

The presence of Co^{2+} at lower concentration made the cathode potential for nickel deposition slightly more noble and thus decreased the cathodic polarization, possibly due to codeposition of cobalt along with nickel. Lowering of the cathode potential during electrodeposition of Co–Ni alloy was also reported by Osman *et al.* [44], Rooksby *et al.* [45] and Halim [46]. The decrease in cathodic polarization of alloy deposition may be due to the decrease in the free energy occurring in the formation of Co–Ni solid solution [40]. On the other hand, at higher Co^{2+} concentration, the cathode potential shifted to a more negative value. The cathodic polarization may be due to a change in the crystal orientation [47]. At lower Co^{2+} concentration crystal growth was favoured in the directions of the (1 1 1) and (2 2 0) planes, whereas at higher concentration the growth was promoted only in the direction of the (2 2 0) plane. The presence of Cu^{2+} in the nickel bath did not show any shift in cathode potential for electrodeposition of nickel. Fig. 4 shows the polarization behaviour of nickel deposition in the presence of 5 to 100 p.p.m. of Fe^{2+}. The cathode potential shifted towards more negative values at all the Fe^{2+} concentrations studied. This phenomenon may be attributed to the anomalous codeposition of iron with nickel [40]. The effect of Fe^{3+} (50–250 p.p.m.) on the polarization characteristics of nickel deposition are shown in Fig. 5. At all the Fe^{3+} concentrations the cathode potential shifted towards more positive values thus showing cathodic depolarization. This may be due to the reduction of Fe^{3+} to Fe^{2+} at the cathode surface for which the reduction potential is much nobler than nickel deposition. It was observed that shifting of cathode potential was in general accompanied by change in deposit purity, crystallographic orientation and surface morphology of the deposit in the presence of all the impurities. In the case of Cu^{2+}, although no change in cathode potential for nickel electrodeposition was observed, marked changes in the physical appearance, purity, orientation and morphology of the deposit were observed at all the concentrations studied.

4. Correlation among various factors

In the case of electrowinning of zinc it has been reported

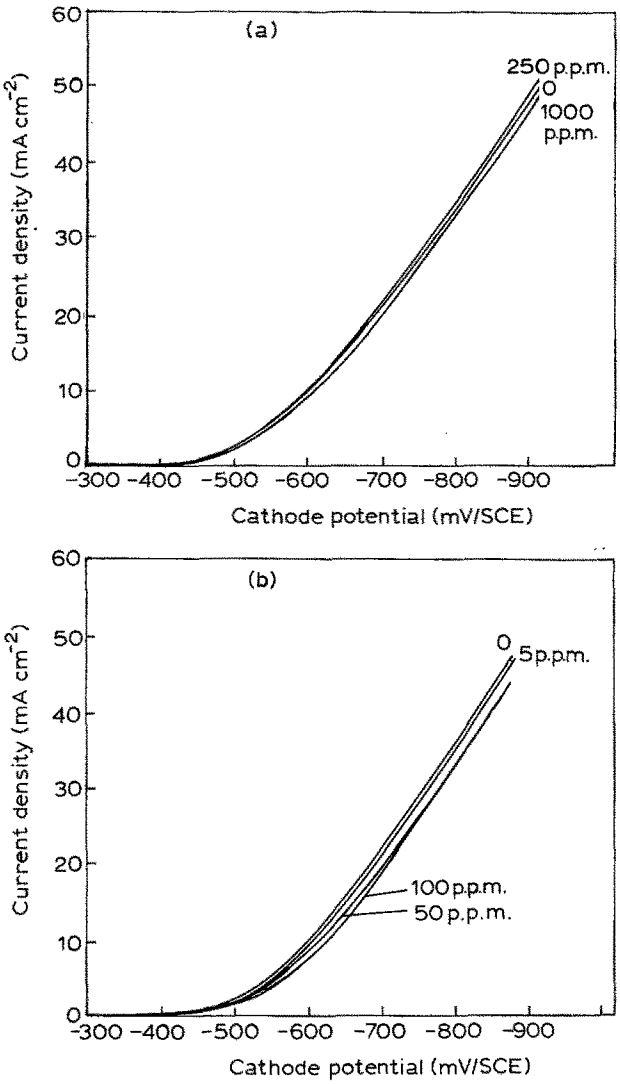

Fig. 4. Potentiodynamic scan curves (1 mV s^{-1}) in NiSO electrolyte containing different concentrations of Co^{2+} and Fe^{2+} at pH 2.0: (a) Co^{2+} and (b) Fe^{2+}.

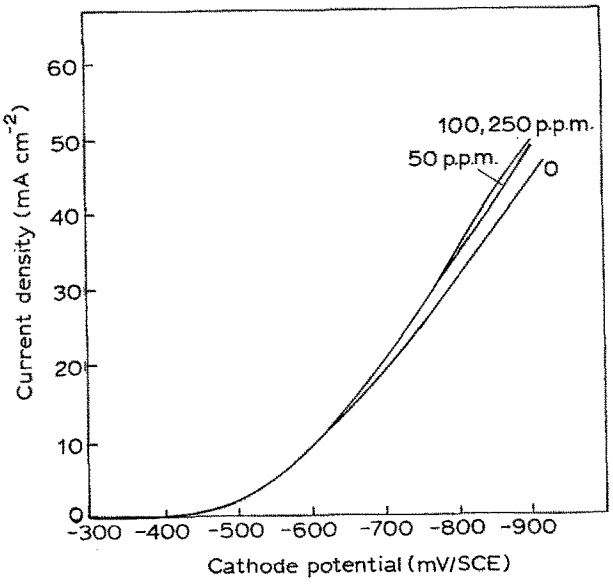

Fig. 5. Potentiodynamic scan curves (1 mV s^{-1}) in $NiSO_4$ electrolyte containing different concentrations of Fe^{3+} at pH 2.0.

Table 5. Relationship among polarization behaviour, tolerance limits and purity of electrodeposited nickel

Impurities	*Nature of polarization*	*Tolerance limits (p.p.m.)*	*Contamination (%)*
Co^{2+}	Depolarization	500	1.72
Cu^{2+}	No polarization	100	0.048
Fe^{2+}	Polarization	5	0.02

[47–49] that there is a relation among polarization behaviour, crystallographic orientation, surface morphology and current efficiency. A similar relationship among these various factors was also observed by Das and Gogia [37] during electrowinning of nickel in the presence of certain impurities. From the present data it seems that, in general, there exists a good relation among the various factors studied, such as deposit purity, crystallographic orientation, surface morphology and polarization behaviour for the electrodeposition of nickel in the presence of Co^{2+}, Cu^{2+}, Fe^{2+} and Fe^{3+}, because any change in any of the factors studied was, in general, reflected on the rest of the factors. There also exists a relationship among polarization behaviour, tolerance limit and deposit purity for the bivalent impurities studied (Table 5). According to the results listed in Table 5, it is observed that the greater the polarization the less is the tolerance limit and the contamination.

5. Conclusions

The effects of Co^{2+}, Cu^{2+}, Fe^{2+} and Fe^{3+} on the physical appearance purity, current efficiency, crystallographic orientations and surface morphology of nickel deposits and on the polarization behaviour during nickel deposition were determined. Based on the results the following conclusions are drawn:

1. The current efficiency decreased in the presence of any of the impurities studied.

2. The deposit purity changed on addition of the impurities to the nickel bath and the effects were more pronounced on increase of their concentrations. The physical appearance of the deposit changed after a certain concentration of the impurities in the bath.

3. The tolerance limits (based on physical appearance of the deposit) was maximum (500 p.p.m.) in the case of Co^{2+} and minimum (5 p.p.m.) in the case of Fe^{2+}.

4. The purity of the electrodeposited nickel was least in the presence of Co^{2+} but highest in the presence of Fe^{2+}.

5. No deviation of nickel structure from fcc was observed in the presence of the impurities studied. However, the peak height values showed variations in the presence of all the impurities and these varied when the impurity concentrations were changed.

6. The surface morphology of the nickel deposit showed variations along with the changes in the crystallographic orientations.

7. The potentiodynamic scan curves for electrowinning of nickel also showed deviations in the presence of all the impurities except Cu^{2+}. Any change in the polarization behaviour was reflected in the deposit purity, crystallographic orientation and surface morphology of the deposits.

8. In general, there exists a relationship among polarization behaviour, crystallographic orientation, purity, physical appearance of the deposit and surface morphology of electrodeposited nickel in the presence of any of the impurities studied.

9. A relationship also exist among polarization behaviour, tolerance limits and purities for the bivalent impurities studied.

Acknowledgements

We are grateful to Dr R. P. Das, Project Coordinator, Hydro & Electrometallurgy Group, for his valuable suggestions and discussion. We particularly wish to acknowledge Professor P. K. Jena, Director, Regional Research Laboratory, Bhubaneswar, for his encouragement and for permission to publish this paper. We also acknowledge Dr B. S. Acharya at RRL-Bhubaneswar for XRD scanning of nickel samples and discussions and Mr. G. Sunder Rao of DMRL-Hyderabad for his SEM examinations of the samples.

References

[1] O. Essin and E. Alfimova, *Trans. Electrochem. Soc.* **68** (1935) 417.
[2] V. Yuza and L. Kopyl, *J. Phys. Chem. USSR.* **14** (1940) 1071.
[3] F. Salt, *Disc. Faraday Soc.* **1** (1947) 169.
[4] A. Gorbachev and Y. Yurkevich, *J. Chem. Phys. USSR.* **28** (1954) 1120.
[5] H. Fischer, M. Seipt and G. Morolock, *Z. Elektrochem.* **59** (1955) 440.
[6] L. Yang, *J. Electrochem. Soc.* **97** (1950) 241.
[7] G. Clark and S. Simonson, *ibid.* **98** (1951) 110.
[8] M. R. F. Wyllie, *J. Chem. Phys.* **16** (1948) 52.
[9] D. J. Evans, *Trans. Faraday, Soc.* **54** (1958) 1086.
[10] D. R. Cliffe and J. P. G. Farr, *J. Electrochem. Soc.* **111** (1964) 299.
[11] I. Epelboin, M. Froment and G. Maurin, *Plating* **56** (1969) 1356.
[12] A. D. K. Reddy, *J. Electroanal. Chem.* **6** (1973) 141, 153, 159.
[13] M. A. Zhamagortsyan, Z. N. Pilikyan, A. A. Yavich and A. T. Vagramyan, *Elektrokhimiya* **11** (1975) 437.
[14] J. Amblard, M. Froment and N. Spyrellis, *Surf. Tech.* **5** (1977) 205.
[15] J. Amblard, I. Epelboin, M. Froment and G. Maruin, *J. Appl. Electrochem.* **9** (1979) 233.
[16] S. Nakahara and E. C. Felder, *J. Electrochem. Soc.* **124** (1982) 45.
[17] A. Vertes, I. Czako Nagy and L. Lakatos-varsenyi, *ibid.* **131** (1984) 1526.
[18] A. W. Hothersall and G. E. Gardam L, *J. Electrodepositor's Tech. Soc.* **15** (1939) 127.
[19] H. Fischer and H. Barmann, *Z. Metallkunde,* **32** (1940) 376.
[20] W. Hume-Rothery and M. R. Wyllie, *Proc. Roy. Soc. Lond.* **A181** (1943) 331.
[21] W. Smith, J. H. Keeler and H. J. Read, *Plating* **36** (1949) 355.
[22] G. L . Clark and S. H. Simonsen, *J. Electrochem. Soc.* **98** (1951) 110.
[23] R. Weil and R. Paquin, *ibid.* **107** (1960) 87.
[24] M. R. Thomson, *Trans. Am. Electrochem. Soc.* **42** (1922) 79.

[25] M. R. Thomson and C. T. Thomas, *ibid.* **42** (1942) reprint.
[26] L. M. Evalnnikov and D. S. Neiman, Leningrad Ind. Inst. No. 1, *Sec. Met. No. 1* (1939) 3.
[27] M. B. Diggin, *Monthly Rev. Am. Electroplater's Soc.* **33** (1946) 513, 524.
[28] Cosimo Quattrone, *Galvanotecnica* **3** (1952) 105.
[29] D. T. Ewing, A. A. Brouwer and J. K. Werner, *Plating* **39** (1952) 1343.
[30] B. C. Banerjee and A. Goswani, *J. Electrochem. Soc.* **106** (1959) 590.
[31] A. Geneidy, W. A. Koehler and W. Machu, *ibid.* **106** (1959) 394.
[32] J. K. Dennis and J. J. Fuggles, *Trans. Inst. Met. Fin.* **46** (1968) 185.
[33] F. E. Lowenheim, 'Modern Electroplating', John Wiley and Sons, New York (1974) pp. 39 and 325.
[34] L. C. Singh, V. B. Singh and P. K. Tikoo, *J. Electrochem. Soc. Ind.* **28** (1974) 87.
[35] W. G. Sherwood, P. B. Queneau, C. Nikolic and D. R. Hodges, *Met. Trans.* **10B** (1979) 659.
[36] W. Blum and G. B. Hogaboom, 'Principles of Electroplating and Electroforming', McGraw-Hill, New York (1949) p. 370.
[37] S. K. Gogia and S. C. Das, *Met. Trans.* **19B** (1988) 6.
[38] J. W. Mellor, 'A Comprehensive Treatise on Inorganic and Theoretical Chemistry', Vol. XV, Longmans, London (1961) p. 35.
[39] D. R. Srivastava and K. S. Nigam, *Surf. Tech.* **10** (1980) 343.
[40] A. Brenner, 'Electrodeposition of Alloys' Vol. 1, Academic Press, New York (1963) pp. 77, 177, 185, 191, 343.
[41] H. Dahms, *J. Electroanal. Chem. Interfacial Electrochem.* **8** (1964) 5.
[42] H. Dahms and I. M. Croll, *J. Electrochem. Soc.* **112** (1965) 771.
[43] M. J. Nicol and H. I. Philip, *J. Electroanal. Chem. Interfacial Electrochem.* **70** (1976) 233.
[44] Sayed, S. Abd El-Rehim, Abd El-Halim, M. El-Halim and Magda, M. Osman, *J. Chem. Tech. Biotech.* **35A** (1985) 415.
[45] J. W. Cuthbertson, N. Parkinson and H. P. Rooksby, *J. Electrochem.* **100** (1953) 107.
[46] Abd El-Halim, M., *Surf. Technol.* **23** (1984) 203.
[47] V. I. Lakshmanan, D. J. Mackinnon and J. M. Brannen, *J. Appl. Electrochem.* **7** (1977) 81.
[48] D. J. Mackinnon and J. M. Brannen, *ibid.* **9** (1979) 71.
[49] B. K. Thomas and D. J. Fray, *J. Appl. Electrochem.* **11** (1981) 677.